NEBRASKA
Good Life. Great Journey.
DEPARTMENT OF TRANSPORTATION

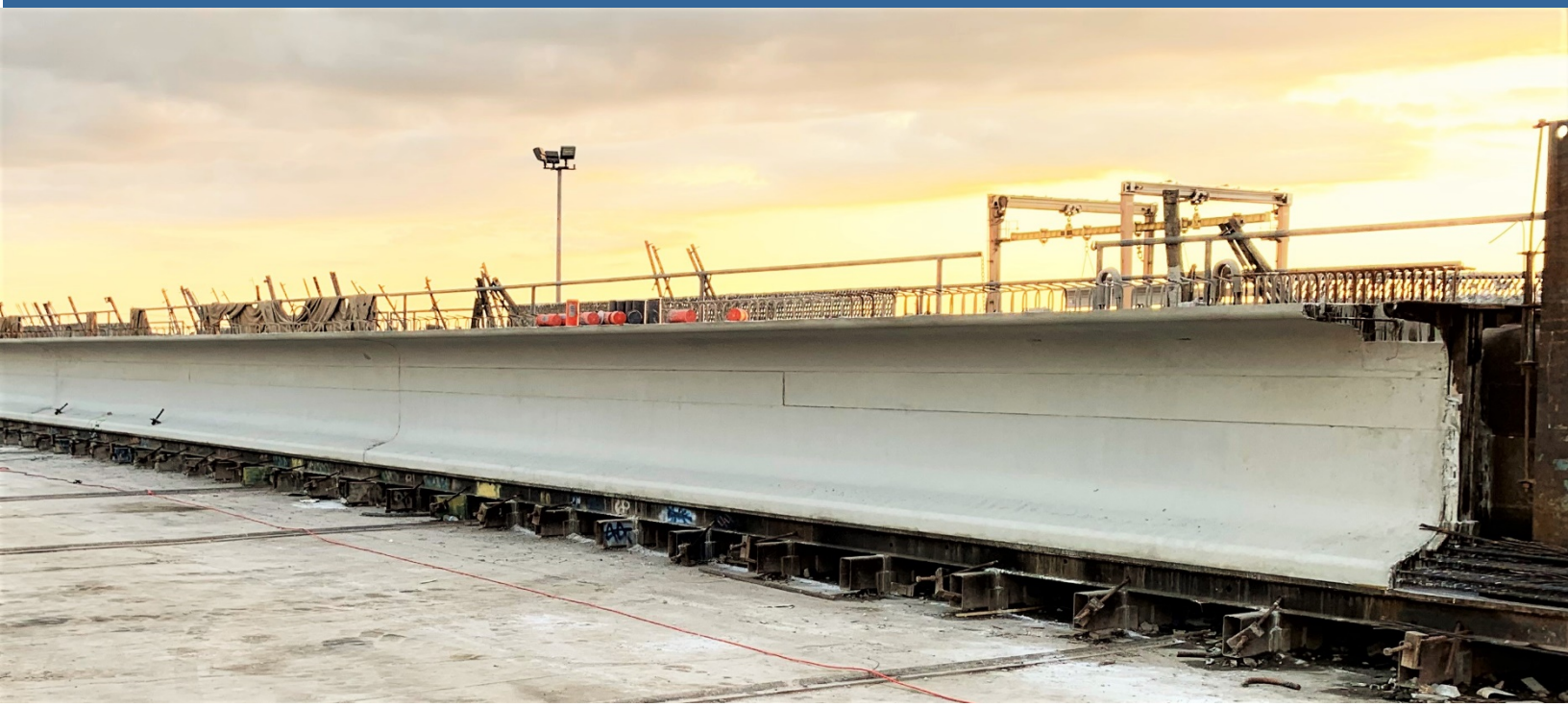

Report SPR-P1(17) M074

Development of an NDT tool for in-situ assessment of prestress loss

Bibo Zhong, Jinying Zhu, George Morcous

Department of Civil Engineering
University of Nebraska-Lincoln

January 2020

TECHNICAL REPORT DOCUMENTATION PAGE

1. Report No. M074	2. Government Accession No.	3. Recipient's Catalog No.
4. Title and Subtitle Development of an NDT Tool for in-Situ Assessment of Prestressed Loss		**5. Report Date** January 2020
		6. Performing Organization Code
7. Author(s) Bibo Zhong, Jinying Zhu, George Morcous		**8. Performing Organization Report No.**
9. Performing Organization Name and Address Department of Civil and Environmental Engineering. University of Nebraska-Lincoln 1110 S 67th St., Omaha, NE 68182		**10. Work Unit No.**
		11. Contract SPR-P1(17) (M074)
12. Sponsoring Agency Name and Address Nebraska Department of Transportation Research Section 1400 Hwy 2 Lincoln, NE 68502		**13. Type of Report and Period Covered** Final Report July 2017 – January 2020
		14. Sponsoring Agency Code
15. Supplementary Notes		

16. Abstract

The research objective is to develop a non-destructive testing (NDT) method to evaluate the prestress loss in prestressed concrete bridge girders using ultrasonic waves. The work principle is based on acoustoelastic effect - ultrasonic wave velocity varies with stress level in prestressed concrete. A self-reference test setup was proposed to measure wave velocity in two orthogonal directions (prestress and unstressed directions) in the girder. This setup will be able to reduce effects of material variation and temperature change.

The concept was first validated on small concrete specimens (cylinders and beams) in laboratory. A signal analysis algorithm was developed to reliably measure P wave velocity change with stress, i.e. the acoustoelastic coefficient. Then the proposed technique was applied to a full-scale prestressed concrete bridge girder (131 ft long) to monitor the stress release process. The stress change monitored by the ultrasonic test showed good agreement with the result from the strain measurement. In both the small beam test and the large girder test, the measured acoustoelastic coefficients were in the range of 0.7%/ksi.

The temperature effects on acoustoelastic coefficient were investigated on two prestressed concrete members. Experimental results showed a slight difference between temperature induced velocity changes in the prestress and unstressed directions. Although temperature variation can cause large change of velocity, the self-reference setup will be able to correct about 80% of temperature effect. The relationship between relative wave velocity changes and stress changes in two orthogonal directions after temperature correction can be used to predict the stress level in concrete and reduce environmental influences.

17. Key Words	18. Distribution Statement
Ultrasonic, Presstress loss, Concrete, Girder	No restrictions. This document is available through the National Technical Information Service. 5285 Port Royal Road Springfield, VA 22161

19. Security Classification (of this report)	20. Security Classification (of this page)	21. No. of Pages	22. Price
Unclassified	Unclassified	45	

Form DOT F 1700.7 (8-72) Reproduction of completed page authorized

DISCLAIMER

The contents of this report reflect the views of the authors, who are responsible for the facts and the accuracy of the information presented herein. The contents do not necessarily reflect the official views or policies neither of the Nebraska Department of Transportations nor the University of Nebraska-Lincoln. This report does not constitute a standard, specification, or regulation. Trade or manufacturers' names, which may appear in this report, are cited only because they are considered essential to the objectives of the report.

The United States (U.S.) government and the State of Nebraska do not endorse products or manufacturers. This material is based upon work supported by the Federal Highway Administration under SPR-1(##) (M##). Any opinions, findings and conclusions or recommendations expressed in this publication are those of the author(s) and do not necessarily reflect the views of the Federal Highway Administration."

Abstract

The research objective is to develop a non-destructive testing (NDT) method to evaluate the prestress loss in prestressed concrete bridge girders using ultrasonic waves. The work principle is based on acoustoelastic effect - ultrasonic wave velocity varies with stress level in prestressed concrete. A self-reference test setup was proposed to measure wave velocity in two orthogonal directions (prestress and unstressed directions) in the girder. This setup will be able to reduce effects of material variation and temperature change.

The concept was first validated on small concrete specimens (cylinders and beams) in laboratory. A signal analysis algorithm was developed to reliably measure P wave velocity change with stress, i.e. the acoustoelastic coefficient. Then the proposed technique was applied to a full-scale prestressed concrete bridge girder (131 ft long) to monitor the stress release process. The stress change monitored by the ultrasonic test showed good agreement with the result from the strain measurement. In both the small beam test and the large girder test, the measured acoustoelastic coefficients were in the range of 0.7%/ksi.

The temperature effects on acoustoelastic coefficient were investigated on two prestressed concrete members. Experimental results showed a slight difference between temperature induced velocity changes in the prestress and unstressed directions. Although temperature variation can cause large change of velocity, the self-reference setup will be able to correct about 80% of temperature effect. The relationship between relative wave velocity changes and stress changes in two orthogonal directions after temperature correction can be used to predict the stress level in concrete and reduce environmental influences.

Acknowledgments

This research project would not have been possible without the funding provided by the Nebraska Department of Transportation. The authors would also like to acknowledge Coreslab Structures Inc. (Omaha site) for providing access and assisting in the test of the full scale bridge girder.

Contents

1 Introduction **1**

1.1 Introduction 1

1.2 Objectives 2

1.3 Report overview 3

2 Literature review and theoretical background **4**

2.1 Literature review 4

2.2 Acoustoelastic effect 8

2.3 Measurement of relative velocity change 9

3 Laboratory experiments **11**

3.1 Ultrasonic sensors selection 11

3.2 Laboratory test plans and experimental setup 13

3.2.1 Laboratory test plans 13

3.2.2 Experimental setup 13

3.3 Analysis of time window effects 15

3.3.1 Time window effects on CWI analysis 15

3.3.2 Time window of direct P wave 17

3.3.3 Automatic determination of P wave arrival 18

3.4 Results from small concrete beam 19

4 Test on a full-scale bridge girder **21**

4.1 Bridge girder description and experimental setup 21

4.2 Results and discussion 22

4.2.1 Ultrasonic monitoring 22

4.2.2 Stress and strain measurements 23

4.3 Temperature effect in prestressed concrete members 25

4.3.1 prestressed concrete specimens and test setup 25
4.3.2 Results of temperature effect 28

5 Conclusions and future work **30**

List of Figures

1.1 Current methods for measuring prestress loss: a) embedded gauges, and b) surface gauges. 2

1.2 (a) Concept of ultrasonic testing for stress evaluation in a prestressed concrete beam. (b) ultrasonic sensor holder to ensure consistent measurement. . 3

2.1 (a) Test setup for measuring acoustoelastic coefficient in concrete, where two ultrasonic transducers are installed on top and bottom ends, and compression load is applied in vertical direction [3]; (b) velocity changes in parallel and transverse directions under axial compression [3]. 5

2.2 Experimental setup of investigating the thermal effect on ultrasonic wave velocity change. Left figure presents the climate chamber with samples equipped with embedded ultrasonic sensors. Right figure shows the velocity variation due to temperature change in three samples [13]. 7

2.3 Temperature compensation by experimenting on two test specimens simultaneously [7]. 7

2.4 An example of applying stretching technique on ultrasonic waveforms. Blue line is acquired from stress-free state, and the red solid line is from unstressed state. The red dash line is interpolated from stressed state waveform at $t(1 + \varepsilon_{max})$. The stretched waveform almost overlaps the reference one. 10

3.1 Strong cross talk in PZT receiver signal. 12

3.2 Selected ultrasonic sensors: (a) PZT sensor from Steminc Inc. (b) AE sensor R61-AST from Physical Acoustic (Mistras). 12

3.3 A typical ultrasonic signal received in the parallel direction on a concrete cylinder. (a) Time domain signal and (b) amplitude spectrum. 13

3.4 Experimental setup of 6" × 12" concrete cylinder. 14

3.5 Experimental setup of the 6" × 6" × 20" concrete beam: (a) side view; (b) plan view. 15
3.6 Signals received from parallel receiver (top plot) and perpendicular receiver (bottom plot). The signals are divided into seven time windows. P wave part is selected at $[t_p, 1.5t_p]$ in this study. 16
3.7 Acoustoelastic coefficients α by stretching different time windows and by stretching the full-length signals. 16
3.8 Sketch of propagation paths of direct P wave (solid line) and coda wave (dash line). 18
3.9 The relationship between wave velocity change and stress in directions parallel to and perpendicular to the stress. 18
3.10 P wave arrival's pickup using AIC method. 19
3.11 Relative P wave velocity change vs. stress on the top surface of the 6" × 6" × 20" concrete beam. 20

4.1 Side view of the 131' prestressed concrete bridge girder (not to scale). . . . 22
4.2 Cross sections at the end (left) and middle (right) of the prestressed concrete bridge girder. 22
4.3 Ultrasonic sensors (top) and DEMC target positions (bottom) on the bridge girder. 23
4.4 Relative velocity change monitored during the prestress release process on the 131-ft long bridge girder, before and after temperature correction. Blue lines represent the result from the parallel receiver, and the red lines are from the perpendicular receiver. The inset in (b) shows more details in the process of cutting the top strands. 24
4.5 Prestress loss calculation based on AASHTO specifications. 26
4.6 Investigating temperature effect on ultrasonic wave velocity in the bridge girder. 27
4.7 Test on an one-way prestressed concrete slab in PKI structural laboratory to investigate the temperature effect on the ultrasonic wave velocity in prestressed concrete members. 28
4.8 Relative velocity change with temperature on the prestressed concrete bridge girder. 29
4.9 Relative velocity change with temperature on the one-way prestressed concrete slab. 29

List of Tables

2.1 Acoustoelastic constant reported by different experiments[4]. 6

Chapter 1

Introduction

1.1 Introduction

Prestressed/precast concrete girders are the most used superstructure system in highway bridges in Nebraska. Recently, the use of prestressed/precast concrete for deck construction have gained considerable attention of state officials to accelerate bridge construction and reduce maintenance cost. In all prestressed concrete systems, loss of prestress occurs immediately after production (short term) due to elastic shortening and during construction and operation (long term) due to shrinkage and creep of concrete and relaxation of prestressing steel, which are inevitable time-dependent phenomena. Loss of prestressing can also occur due to collision of bridge girders by oversized vehicles, which could result in rupture of few strands. All these effects reduce the pre-compression of the tension fibers of the concrete component and could significantly affect the component performance under service loads resulting in frequent cracking.

AASHTO LRFD Section 5.9.5 "Loss of Prestress" provides two methods for estimating time-depended prestress losses: Approximate Estimate and Refined Estimate. Despite the complexity and accuracy of the refined estimate, the reliability of the predicted losses is still highly dependent on the actual material properties, environmental conditions, and interaction between connected components. Currently, the existing methods for measuring prestress loss require either installation of wired gauges inside the component during production (Figure 1.1a), or installation of surface gauges prior to prestress release (Figure 1.1b) to achieve a zero-stress reference, which are impractical in practice.

Acoustoelastic effect refers to the dependency of ultrasonic wave velocities on stress and polarization in materials. It is a nonlinear effect between stress and strain in an elastic

material. In theory, if the acoustoelastic coefficients (relative velocity change dV/V vs. stress change) that express the linear relationship between ultrasonic velocities and stress state of first order are determined, we can estimate the stress level in materials by measuring ultrasonic velocity variations.

Fig. 1.1. Current methods for measuring prestress loss: a) embedded gauges, and b) surface gauges.

1.2 Objectives

The objective of this research is to develop a self-referenced non-destructive testing (NDT) tool for in-situ stress evaluation of prestressed concrete bridge components. The main advantage of the new tool is that it can be used on the components surface (girder soffit or deck top surface) with no need for reference readings. The conceptual sketch is presented in Figure 1.2 for ultrasonic measurement on the bottom surface of a girder. Two ultrasonic sensors (R1, R2) in orthogonal directions will receive signals emitted from the same ultrasonic transmitter (red circle). Sensor R1 will measure waves that have the same polarization and propagation direction as the prestress (horizontal), and the velocity is affected by the stress level; while R2 will measure waves propagating/polarizing in the unstressed direction (vertical), where the velocity is not or less affected by the prestress. R2 signal can be approximately regarded as the reference signal at unstressed state; and the velocity difference calculated between R1 and R2 signals will be used to evaluate the prestress level. Since the signal under prestress and the reference signal are measured from the same structure at the same time, the self-reference approach will eliminate effects of material and temperature variations.

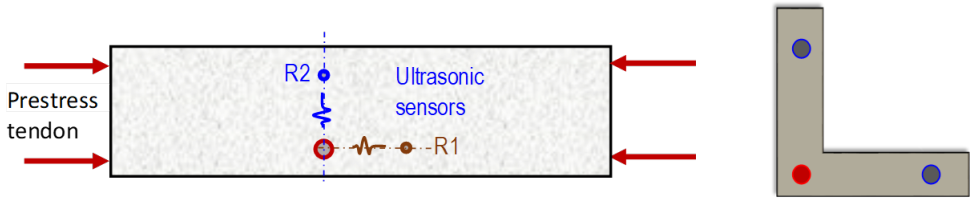

Fig. 1.2. (a) Concept of ultrasonic testing for stress evaluation in a prestressed concrete beam. (b) ultrasonic sensor holder to ensure consistent measurement.

1.3 Report overview

This research project focused on investigating the relationship between stress in concrete and ultrasonic wave velocity change and developing a feasible NDT technique to evaluate the prestress loss in prestressed concrete bridge girder. This research report consists of five chapters. **Chapter** 1 presents the introduction of current prestress loss evaluation methods, and summarizes research objectives. **Chapter** 2 reviews current NDT methods based on acoustoelastic effect for evaluating stress in concrete and their challenges. Related theoretical background is described. **Chapter** 3 presents two laboratory experiments along with the results and discussion. A feasible NDT technique for measuring the stress level is proposed. In **chapter** 4, the developed ultrasonic test method was applied to a 131-foot long prestressed concrete girder at Coreslab Structures in Omaha. The temperature effects on the wave velocity change were also investigated. **Chapter** 5 presents the conclusion of this research project and future work.

Chapter 2

Literature review and theoretical background

2.1 Literature review

Existing techniques for measuring prestress loss can be divided into destructive and non-destructive methods [1, 2]. Current non-destructive methods either require sensors to be embedded in the component during production or request an initial reference value, which is impractical for existing prestressed concrete components.

One promising method is to evaluate the stress in concrete using ultrasonic waves based on the acoustoelastic phenomena [3, 5]. The acoustoelastic effect describes that the wave velocity linearly changes with the stress in concrete [3, 5–7]. Figure 2.1(a) shows a laboratory test setup for measuring ultrasonic wave velocity change in a concrete cylinder under compression test. Figure 2.1(b) presents the test results, which show that the ultrasonic P wave velocity changes 0.13 %/MPa (0.9 %/ksi) when the wave polarization is parallel to the stress direction (Axis 1), while the change in transverse direction (Axis 2) is only 0.02 %/MPa (0.003 %/ksi). These slopes are defined as acoustoelastic coefficients.

Planès and Larose [4] gave a comprehensive review of acoustoelastic coefficients in concrete measured by different researchers. They found the reported acoustoelastic coefficients vary widely, ranging from 0.01 %/MPa (0.07 %/ksi) to 0.5 %/MPa (3.4 %/ksi). The results are summarized in Table 2.1. In these experiments, researchers calculated the wave velocity change either by picking up the first arrival time of ultrasonic wave or using the coda wave interferometry (CWI) analysis. Since the velocity change is very small for acoustoelastic effect, the first arrival method does not provide sufficient accuracy and is

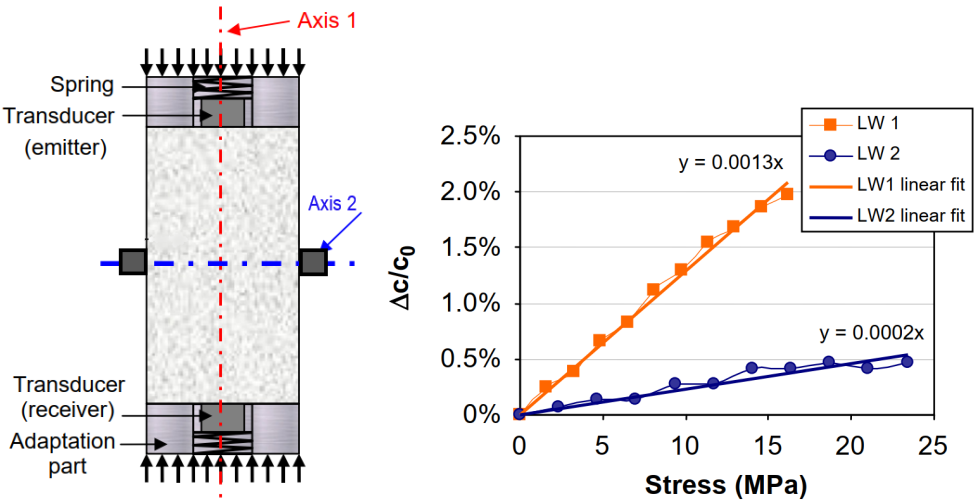

Fig. 2.1. (a) Test setup for measuring acoustoelastic coefficient in concrete, where two ultrasonic transducers are installed on top and bottom ends, and compression load is applied in vertical direction [3]; (b) velocity changes in parallel and transverse directions under axial compression [3].

prone to errors. Alternatively, the CWI analysis method calculates the velocity change [6–9] using cross correlation between the reference and perturbed signals. The CWI analysis has very high sensitivity to a small velocity change in materials by using the entire signal or a segment of signal. A challenge in CWI analysis is how to select the signal window. Zhang et al. [7] suggests that the start time of the window needs to be late enough so that the ultrasonic propagation distance is greater than four times the transport mean free path l^* [10]. However, it is still found that the acoustoelastic constants vary depending on the selected time window in the signals [7, 11]. More details about CWI analysis are presented in section 2.3.

Unlike experiments in the laboratory which is under relatively stable temperature environment, actual prestressed concrete bridges experience a wide range of temperature changes. Many studies indicate that the temperature change has quite significant effect on the ultrasonic wave velocity in concrete [7, 12–15]. Figure 2.2 presents an experimental study about the temperature effect on the wave velocity change in concrete. The velocity changes about 4% in a 50°C range, which corresponds to a velocity change rate of 0.08%/°C. Most concrete structures experience more than 20°C temperature change daily. Therefore, the thermal induced velocity change is comparable to or much larger than the acoustoelastic effect (about 0.1%/MPa). One solution to the temperature effect problem is

Table 2.1. Acoustoelastic constant reported by different experiments[4].

Test configuration	Acousto-elastic constant (A_{ij})	Specification
Uni-axial load	10^{-3} MPa^{-1}	
Uni-axial load	10^{-4} to 10^{-3} MPa^{-1}	dePends on wave polarization
Uni-axial load	10^{-4} to 10^{-3} MPa^{-1}	Depends on wave polarization, direct wave (no CWI)
Cyclic uni-axial load	2.3×10^{-3} up to 4.6×10^{-3} MPa^{-1}	Increases with damage
Four-point bending test	Not apply	dV/V increases with damage
Uni-axial load	0.5×10^{-3} up to 5.5×10^{-3} MPa^{-1}	A increased with thermal damage
Cyclic uni-axial load	0.7×10^{-3} up to 4×10^{-3} MPa^{-1}	A increased with mechanical damage
Cyclic uni-axial load	0.5×10^{-3} up to 2×10^{-3} MPa^{-1}	A increased with chemical (ASR) damage
Cyclic load	Not apply	Real size structure, dV/V increased with damage
Uni-axial load	0.5×10^{-3} MPa^{-1}	Also tested on a bridge under construction
Uni-axial tensile load	0.93×10^{-3} to 1.1×10^{-3} MPa^{-1}	A slightly increased with a 20 h creep test at 7 MPa

to use a reference specimen for temperature compensation, as shown in figure 2.3. However, this method only works if the reference specimen is exactly the same as the test specimen, which is not available in field applications.

In this study, we will focus on the following problems: (1) verify the acoustoelastic effect in concrete; (2) investigate the time window effect on the CWI analysis; (3) address the temperature effect. This chapter presents the theoretical background of acoustoelastic effect and the CWI analysis method. Experimental studies will be shown in the following chapters.

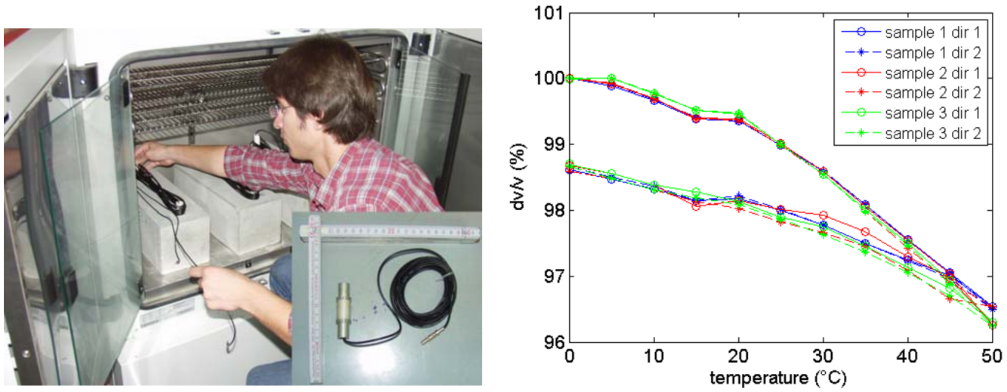

Fig. 2.2. Experimental setup of investigating the thermal effect on ultrasonic wave velocity change. Left figure presents the climate chamber with samples equipped with embedded ultrasonic sensors. Right figure shows the velocity variation due to temperature change in three samples [13].

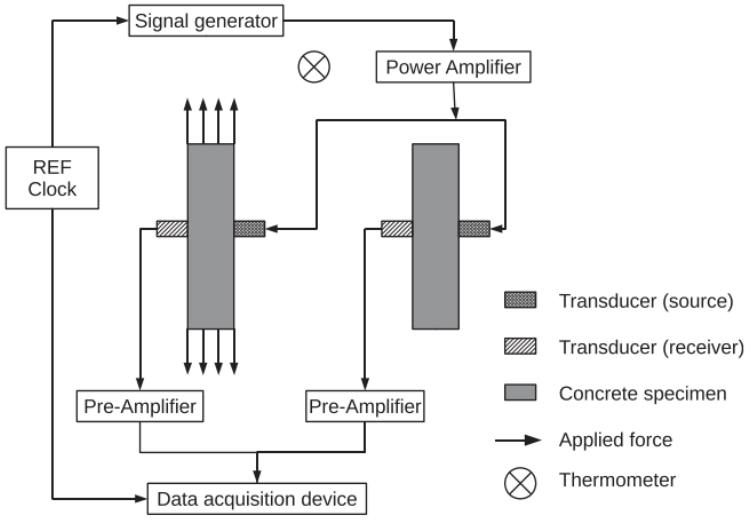

Fig. 2.3. Temperature compensation by experimenting on two test specimens simultaneously [7].

2.2 Acoustoelastic effect

The acoustoelastic effect describes the dependence of the stress wave velocity on the stress/strain in the medium. In 1953, based on Murnaghan's finite deformation theory [16], Hughes and Kelly [17] derived equations describing the relationship between the velocities of elastic waves and the strains in an isotropic body subjected to a homogeneous triaxial finite strain:

$$\rho_0 V_{11}^2 = \lambda + 2\mu + (2l + \lambda)\theta + (4m + 4\lambda + 10\mu)\alpha_1 \tag{2.1a}$$

$$\rho_0 V_{12}^2 = \mu + (\lambda + m)\theta + 4\mu\alpha_1 + 2\mu\alpha_2 - \frac{1}{2}n\alpha_3 \tag{2.1b}$$

$$\rho_0 V_{13}^2 = \mu + (\lambda + m)\theta + 4\mu\alpha_1 + 2\mu\alpha_3 - \frac{1}{2}n\alpha_2 \tag{2.1c}$$

where

$$\begin{aligned}
\rho_0 &= \text{initial density} \\
V_{11}, V_{12}, V_{13} &= \text{velocities of elastic waves propagating in direction 1} \\
&\quad \text{polarizing in direction 1, 2, and 3.} \\
\lambda, \mu &= \text{Lamé constants} \\
l, m, n &= \text{Murnaghan constants} \\
\alpha_1, \alpha_2, \alpha_3 &= \text{homogeneous triaxial finite strain in direction 1, 2, and 3} \\
\theta &= \alpha_1 + \alpha_2 + \alpha_3
\end{aligned}$$

For a state of uniaxial stress in direction 1, the strains are $\alpha_1 = \epsilon$, $\alpha_2 = \alpha_3 = -\nu\epsilon$. When the strain changes are small, the relative wave velocity changes can be expressed as [17, 18]:

$$\frac{dV_{11}/V_{11}^0}{d\epsilon} = 2 + \frac{\mu + 2m + \nu\mu(1 + 2l/\lambda)}{\lambda + 2\mu} \tag{2.2a}$$

$$\frac{dV_{12}/V_{12}^0}{d\epsilon} = 2 + \frac{\nu n}{4\mu} + \frac{m}{2(\lambda + \mu)} \tag{2.2b}$$

$$\frac{dV_{22}/V_{22}^0}{d\epsilon} = -2\nu(1 + \frac{m - \mu l/\lambda}{\lambda + 2\mu}) \tag{2.2c}$$

$$\frac{dV_{21}/V_{21}^0}{d\epsilon} = \frac{\lambda + 2\mu + m}{2(\lambda + \mu)} + \nu n/4\mu \tag{2.2d}$$

$$\frac{dV_{23}/V_{23}^0}{d\epsilon} = \frac{m - 2\lambda}{2(\lambda + \mu)} - \frac{n}{4\mu} \tag{2.2e}$$

These equations are further generalized by Lillamand et al. [3], and the elastic wave velocity under uni-axial loading can be expressed as:

$$V_{ij}^{\sigma} = V_{ij}^{0}(1 + \alpha_{ij}\sigma_{11}) \tag{2.3a}$$

$$\frac{dV_{ij}}{V_{ij}^{0}} = \alpha_{ij}\sigma_{11} \tag{2.3b}$$

where V_{ij}^{σ} is the wave velocity under the uni-axial stress σ_{11}, and V_{ij}^{0} is the wave velocity under stress-free state. dV_{ij} represents the wave velocity change from stress-free state to uni-axial stress σ_{11} state. The subscript ij stands for the wave propagation direction and polarization direction. α_{ij} is defined as the acoustoelstic coefficient which depends on elastic constants (Lamé and Murnaghan), Young's modulus, the wave propagation direction, and the wave polarization direction.

2.3 Measurement of relative velocity change

The reported acoustoelastic coefficients range from 0.01 %/MPa (0.07 %/ksi) to 0.5 %/MPa (3.4 %/ksi) in concrete [3–6]. Conventional ultrasonic test methods by measuring the time of flight (TOF) of P wave, such as the UPV test, cannot achieve such precision.

The stretching technique is a relatively new method used for measurement of relative wave velocity change [19] in CWI analysis. This method assumes the perturbed signal is a uniformly stretched (or compressed) version of the reference signal, so that it stretches (or compresses) the perturbed signal to obtain maximum agreement with the reference signal. In computer program, it first interpolates the perturbed signal S_1 at times $t(1 + \varepsilon)$ with a series of stretching factors ε, and then compare with the reference signal S_0 by using the cross-correlation coefficient:

$$CC(\varepsilon) = \frac{\int_{t_1}^{t_2} S_1[t(1+\varepsilon)]S_0[t]dt}{\sqrt{\int_{t_1}^{t_2} S_1[t(1+\varepsilon)] \int_{t_1}^{t_2} S_0^2[t]dt}} \tag{2.4}$$

where t_1 to t_2 is the selected time window for calculation. The ε_{max} that maximizes the cross-correlation coefficient (CC) can represent the relative wave velocity change $-dt/t$, and the relative wave velocity change $dV/V = -dt/t = \varepsilon_{max}$ [19, 20]. A demonstration of the stretching technique on two ultrasonic waveforms is shown in figure 2.4.

The stretching technique has been widely used to evaluate small ultrasonic velocity changes in concrete. Larose and Hall [6] utilized the stretching technique to reach a

resolution of 2×10^{-5} relative wave velocity change in concrete due to uni-axial stress. Hadziioannou et al. [21] measured the small velocity change in concrete due to the temperature change and found the stretching method is stable even when the signal-to-noise ratio is low. Sun and Zhu [15] developed a nonlinear ultrasonic parameter for concrete damage evaluation by measuring relative velocity changes with temperature. Niederleithinger et al. [22] successfully monitored stress distribution and localized large cracks on a 12 meter (39 ft) long girder.

When using the stretching technique, it is assumed a uniform velocity change in the media, which is valid for uniform temperature change, but not valid in the uni-axial stress condition. After multiple scatterings, the coda waves (late part of signal) contain both P wave and S wave, and the relative velocity change calculated by the CWI analysis is a weighted average of P and S velocity perturbation [23]. Therefore, the relative velocity change through CWI analysis is affected by the chosen time window when the concrete specimen is under uni-axial stress [7, 11].

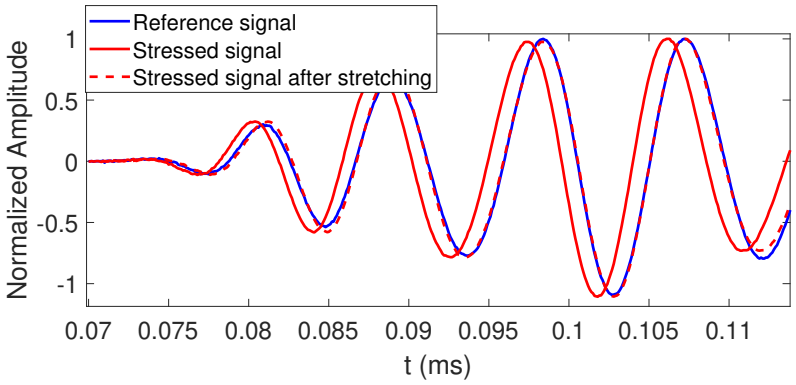

Fig. 2.4. An example of applying stretching technique on ultrasonic waveforms. Blue line is acquired from stress-free state, and the red solid line is from unstressed state. The red dash line is interpolated from stressed state waveform at $t(1 + \varepsilon_{max})$. The stretched waveform almost overlaps the reference one.

Chapter 3

Laboratory experiments

This chapter presents laboratory experiments on concrete cylinders in compression test and on beams in bending test. In both tests, ultrasonic wave velocities were measured along the stress direction and also in the transverse direction. Acoustoelastic coefficients were calculated and compared. In this chapter, sensor selection and signal analysis methods are also discussed.

3.1 Ultrasonic sensors selection

In the experimental study, ultrasonic wave frequency should first be determined. Low-frequency (< 20 kHz) signals have a good signal-to-noise ratio (S/N) and a long propagation distance, but are insensitive to small changes. High-frequency (> 500 kHz) signals can detect very small changes, but they decay quickly, resulting in short propagation distances and low S/N [4]. Fröjd and Ulriksen [24] investigated the frequency influence on CWI analysis in concrete specimens and recommended ultrasonic waves in the frequency range of 50-150 kHz for good sensitivity and S/N.

In this study, we first used PZT disks for the ultrasonic transmitter and the receivers. One challenge for using the PZT sensor is presence of cross talk in signals, as shown in figure 3.1. For a short source-receiver distance, the beginning part of the signal may be mixed with cross talk, which affects CWI analysis.

After investigating different combinations of ultrasonic sources and sensors, we decided to use the PZT disk as the ultrasonic transmitter and acoustic emission (AE) sensors as the ultrasonic receivers, as shown in figure 3.2. This PZT disk is 20 mm in diameter and 3 mm thick and vibrate in thickness mode. The PZT sensor has low cost and low profile and easy

for quick installation. The AE sensor (Mistras R6I) is a resonant type sensor with central frequency of 60 kHz. The AE sensor is used because 1) it has good shielding and can avoid cross talk; 2) the frequency range of R61 sensor is in a proper range for measuring acoustoelastic effect; 3) it has high sensitivity and good S/N. A typical ultrasonic signal and its frequency spectrum are shown in the figure 3.3.

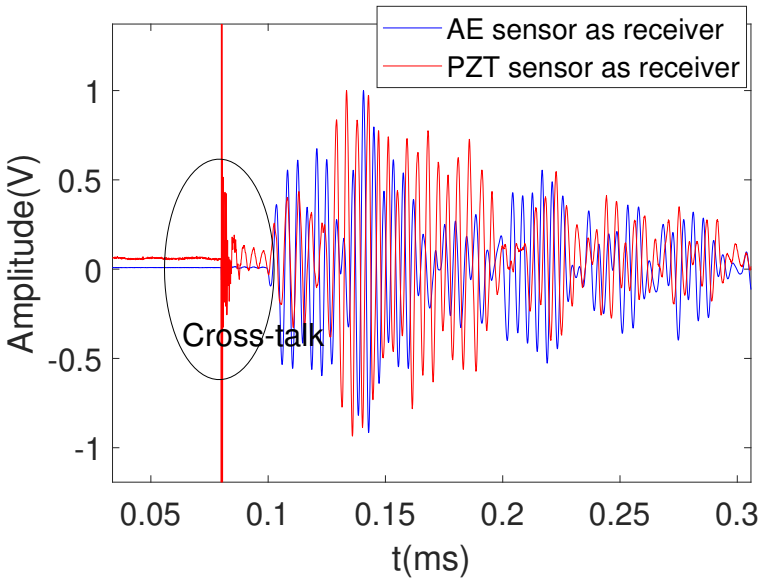

Fig. 3.1. Strong cross talk in PZT receiver signal.

Fig. 3.2. Selected ultrasonic sensors: (a) PZT sensor from Steminc Inc. (b) AE sensor R61-AST from Physical Acoustic (Mistras).

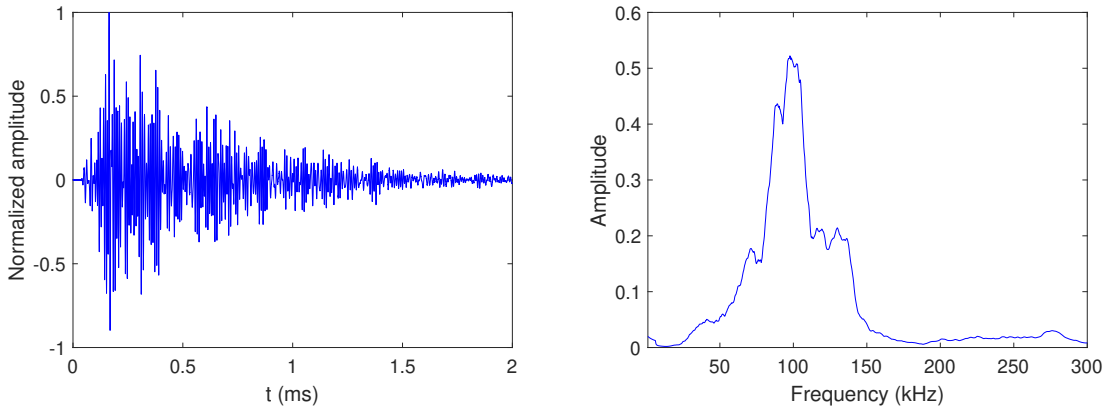

Fig. 3.3. A typical ultrasonic signal received in the parallel direction on a concrete cylinder. (a) Time domain signal and (b) amplitude spectrum.

3.2 Laboratory test plans and experimental setup

3.2.1 Laboratory test plans

The laboratory study include two types of tests and specimens: 1) uni-axial loading test on a 6" × 12" concrete cylinder, and 2) four-point bending test on a 6" × 6" × 20" concrete beam. The compression test on the cylinder was used to investigate the acoustoelastic effect and the time window effect on CWI analysis. The bending test was used to simulate the test on a bridge girder. The specimens in both tests were cast from the same concrete mix batch and have the same material properties. The 28-day compressive strength was 45 MPa (6.5 ksi), and the Young's modulus E = 31 GPa (4496 ksi) which was obtained from the stress-strain curve on a 6" × 12" concrete cylinder.

3.2.2 Experimental setup

The experimental setup on the 6" × 12" concrete cylinder is shown in figure 3.4. A PZT sensor was installed on one side of the cylinder using epoxy and used as an ultrasonic transmitter. Two AE sensors (R61) were used as ultrasonic receivers. One was installed on the opposite side in the transverse direction, and one on the same side of the transmitter in the direction parallel to the stress. The receivers are named as the perpendicular receiver ($\perp$ receiver) and the parallel receiver ($//$ receiver) based on the relative receiver-to-transmitter directions to the stress direction. A load cell was placed under the concrete cylinder to record the loading process.

The ultrasonic setup on the 6" × 6" × 20" concrete beam is similar to the concrete cylinder test, except that ultrasonic transmitter and receivers were placed on the same surface, as shown in figure 3.5. A 120 mm (5") strain gauge was installed between the PZT transmitter and the parallel receiver to monitor strain during the loading process. This setup simulates the situation in field tests because only one surface is typically accessible in bridge girders.

Both tests were performed in a Forney concrete compression/bending machine. In both compression and bending tests, the specimens were loaded at a rate of 4 psi/sec. In the compression test, the load was applied up to 30% of the ultimate load to avoid microcracks in concrete [25]. In the bending test, the load was loaded until the beam failed.

An Olympus 5077PR ultrasonic square wave pulser/receiver was used to drive the PZT transmitter. The pulser duration was set for optimum driving around 100 kHz. The received signals were sampled by a digital oscilloscope PicoScope® 4824 at the sampling rate of 40 MS/s and the duration of each signal was 2 ms. Each signal was averaged ten times to increase the signal-to-noise ratio. The ultrasonic signals were recorded every 2 seconds during the loading process. A LabVIEW program was developed to control the data acquisition system and synchronize ultrasonic data and loading/strain data.

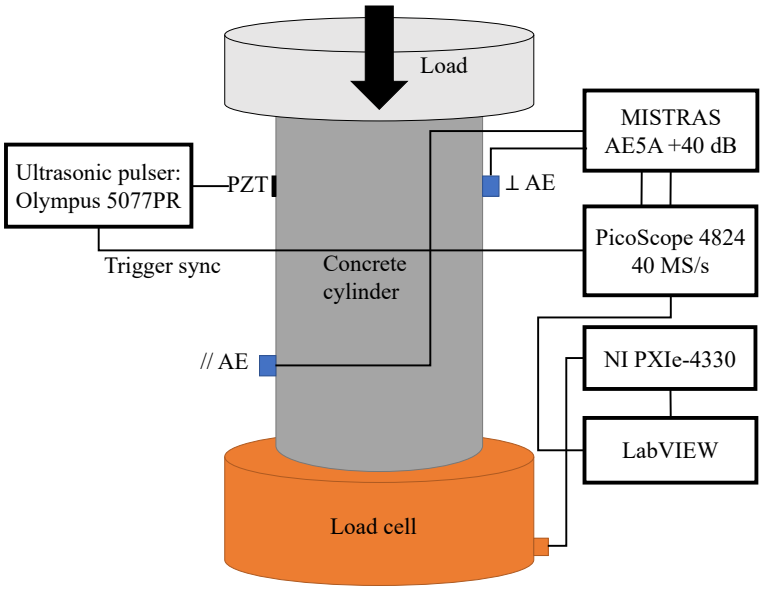

Fig. 3.4. Experimental setup of 6" × 12" concrete cylinder.

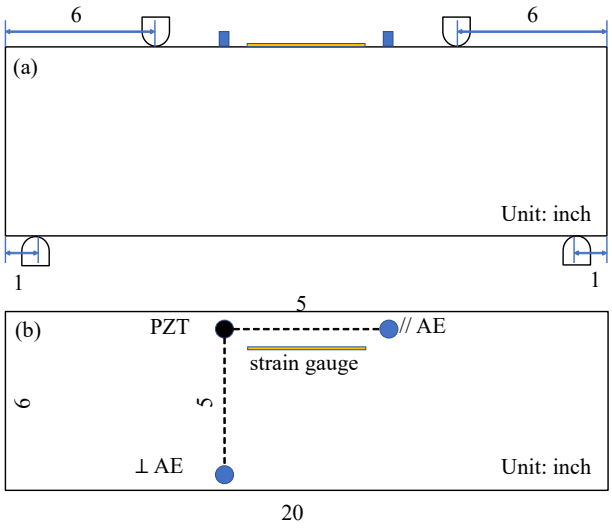

Fig. 3.5. Experimental setup of the 6" × 6" × 20" concrete beam: (a) side view; (b) plan view.

3.3 Analysis of time window effects

3.3.1 Time window effects on CWI analysis

When the CWI analysis method is used to calculate the stress induced velocity change in concrete, many researchers found that the results depend on the chosen time window in the signals [7, 11], which means the material change in concrete is nonuniform. Figure 3.6 shows two signals received from a concrete cylinder in two directions, in which the primary P wave components are highlighted in both signals. The parallel signal has clear P wave and Rayleigh wave arrivals, which are the components propagating along the surface. In order to investigate the time window effects on the acoustoelastic coefficients, the signals were divided into seven time windows and each windowed signal was used to calculate the relative velocity change by the stretching technique, as shown in figure 3.6. The centers of the seven non-overlapping windows (t_c) are from 0.075 ms to 0.975 ms in the first half of the entire signal, and the width of each window (t_w) is 0.15 ms. The acoustoelastic coefficients calculated from these seven windows and the full-length signal are shown in figure 3.7. It can be seen that the calculated acoustoelastic coefficients vary largely with different time windows in both stress direction (// receiver) and unstressed direction (⊥ receiver). The solid lines represent results by stretching the full-length signals, which can be regarded as a weighted average of the values from the seven time windows.

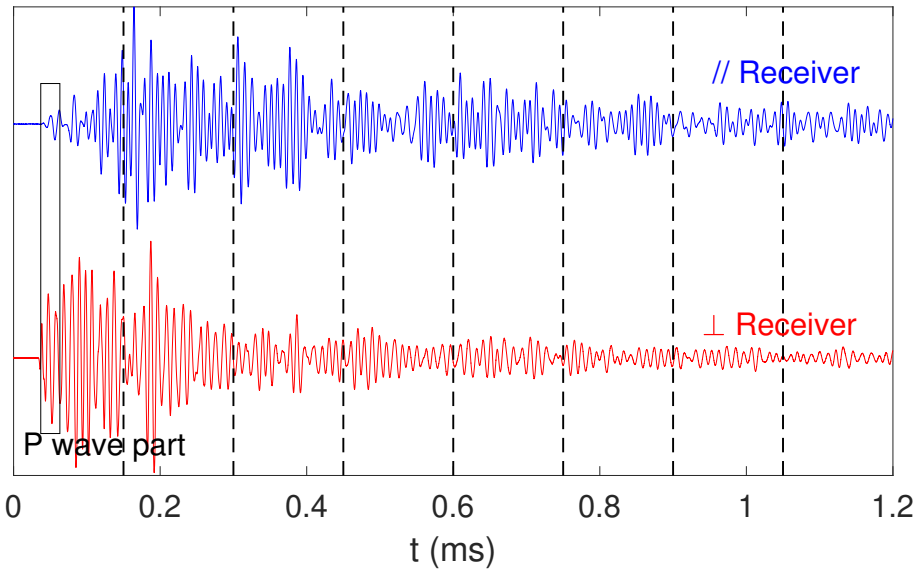

Fig. 3.6. Signals received from parallel receiver (top plot) and perpendicular receiver (bottom plot). The signals are divided into seven time windows. P wave part is selected at $[t_p, 1.5t_p]$ in this study.

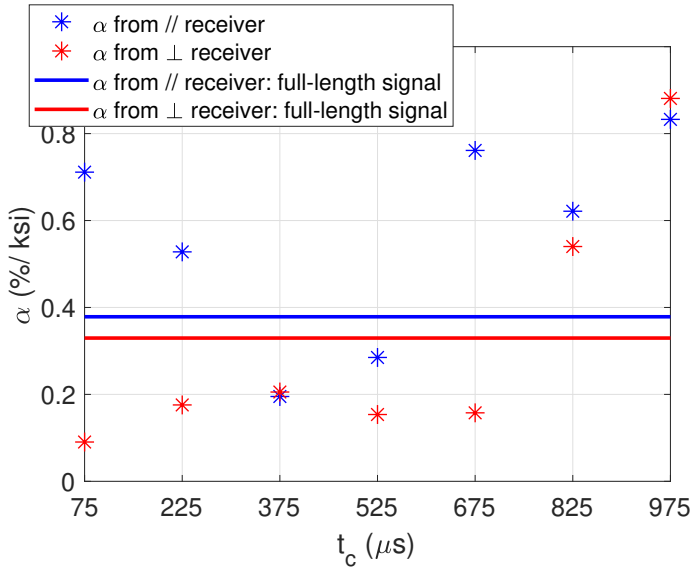

Fig. 3.7. Acoustoelastic coefficients α by stretching different time windows and by stretching the full-length signals.

Lillamand et al. [3], Bompan and Haach [5] found that the acoustoelastic effect is the most significant when the wave propagates and polarizes in the stress direction. Therefore, the wave components mostly propagating in the stress direction show highest velocity change and vice versa. However, if the full-length signals are analyzed, the acoustoelastic coefficients do not show much difference between two directions. In the cylinder test, we obtained $\alpha = 0.055$ %/MPa (0.38 %/ksi) in the parallel direction, and $\alpha = 0.048$ %/MPa (0.33 %/ksi) in the perpendicular direction, respectively. These results can be explained by that after many scatterings, the fully diffused wave has random propagation directions and polarization, and therefore the acoustoelastic coefficients do not depend on the sensor location, as shown in figure 3.8. In this way, the acoustoelastic coefficients calculated from the coda wave parts or the full-length signal do not represent the corresponding acoustoelastic effects in each direction.

3.3.2 Time window of direct P wave

To ensure consistent wave propagation and polarization directions in the measurement, we propose the use of the time window containing the direct P wave part only, as shown in figure 3.6. The selected time window is in the range of $[t_p, 1.5\,t_p]$, where t_p is the arrival time of the P wave. Because the velocity ratio between P and S waves is $V_s/V_p \approx 0.6$, we choose $1.5\,t_p$ as the end of P wave window to avoid the S wave's arrival. Unlike the coda wave, the time window $[t_p, 1.5\,t_p]$ contains only the direct P wave. As seen in figure 3.8, the coda wave experiences much longer travel path than the direct P wave, and has random propagation/polarization directions. In this test setup, the direct P waves follow either the stress direction or unstressed direction. By using the time window at $[t_p, 1.5\,t_p]$, the propagation and polarization of ultrasonic waves can be fixed along the stress direction and unstressed direction, avoiding the mixing of other wave types.

Figure 3.9 shows the relationship between relative velocity change and stress level calculated from the time windowed signals in $[t_p, 1.5\,t_p]$ and the full-length signals in two directions. The velocity change of direct P wave in the parallel direction shows a much higher sensitivity than in the perpendicular direction. In the parallel direction, both the propagation and the polarization directions of the direct P wave are along with the stress, whereas in the perpendicular direction, the propagation and polarization directions are perpendicular to the stress direction. When the full signals are analyzed, the coefficients are similar in both directions.

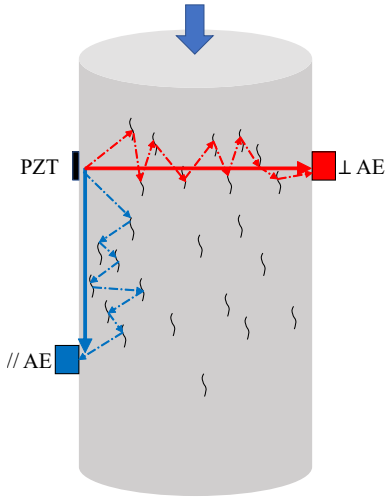

Fig. 3.8. Sketch of propagation paths of direct P wave (solid line) and coda wave (dash line).

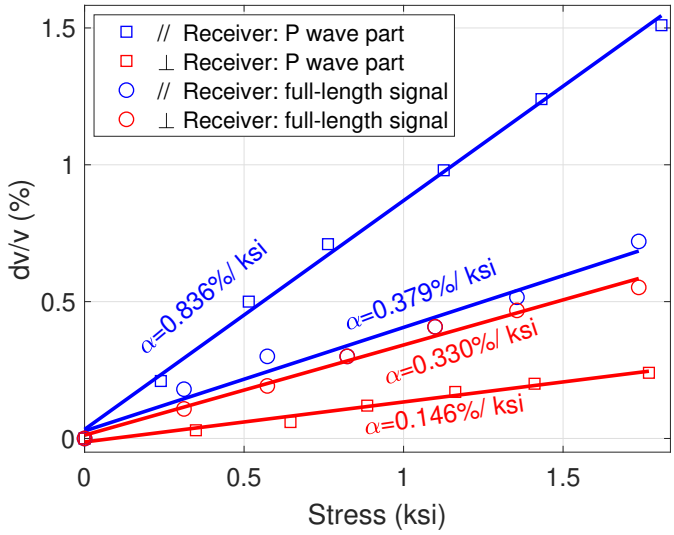

Fig. 3.9. The relationship between wave velocity change and stress in directions parallel to and perpendicular to the stress.

3.3.3 Automatic determination of P wave arrival

In the time window selection process, the P wave arrival time t_p was manually picked. To improve the efficiency of data processing and reduce manual error, the Akaike Information Criteria (AIC) method [26–28] is used to roughly determine the P wave arrival time t_p. For

a digital waveform $S[1, N]$ of length N samples, the AIC value is evaluated as:

$$AIC(k) = k \log[\mathrm{Var}(S[1, k])] + (N - k - 1) \log[\mathrm{Var}(S[k + 1, N])] \tag{3.1}$$

where k is the k^{th} sample of the signal, and Var() is the variance function. In the analyzed time window, the global minimum of AIC value can represent the onset point t_p. Figure 3.1 shows an example of P wave arrival pickup using the AIC method.

Because the relative wave velocity change due to stress is very small, the AIC method is only used to approximate t_p and the time window rather than calculate the relative wave velocity change. The AIC method will be used in all following experiments to determine the time window.

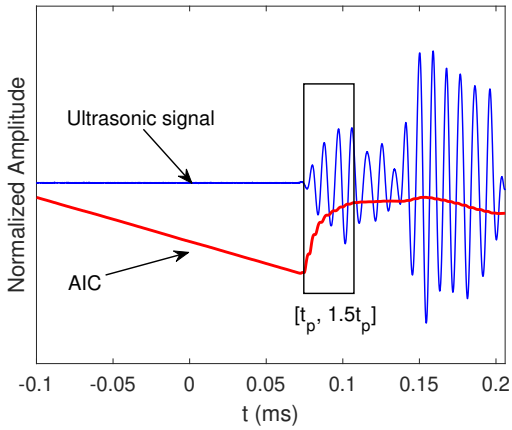

Fig. 3.10. P wave arrival's pickup using AIC method.

3.4 Results from small concrete beam

Similar test and data analysis procedures were also applied to the bending test on the small concrete beam (6" × 6" × 20"). Figure 3.11 presents the relative velocity change of P wave along the stress direction and stress free direction, by stretching the signals in the window of $[t_p, 1.5\,t_p]$. Along the stress direction, the acoustoelastic coefficient is 0.768 %/ksi, slightly smaller than the value measured in the cylinder test (0.836 %/ksi). In the transverse direction (stress free), the P wave velocity slightly decreases with increasing stress level, whereas the velocity still increases in the concrete cylinder test. The authors believe that the difference is caused by different lateral confinement conditions in the beam and cylinder

tests. In the cylinder test, the circumferential restraint results in compressive stress in the transverse direction [29, 30], which causes increasing velocity with loading. However, in the bending test of the concrete beam, the transverse direction is free to expand due to the Poisson's effect, which causes small decrease of P wave velocity in the lateral direction. We expect a similar behavior in the two directions on large prestressed concrete girders.

In field tests, no reference signal from the zero stress state is available. With the self-reference test setup, we can use the measurement in the lateral direction as the reference, and estimate the stress level based on velocity difference between two directions. The self-reference method can also reduce the effects of concrete material variation and temperature changes. More details on the temperature effects are presented in the next chapter.

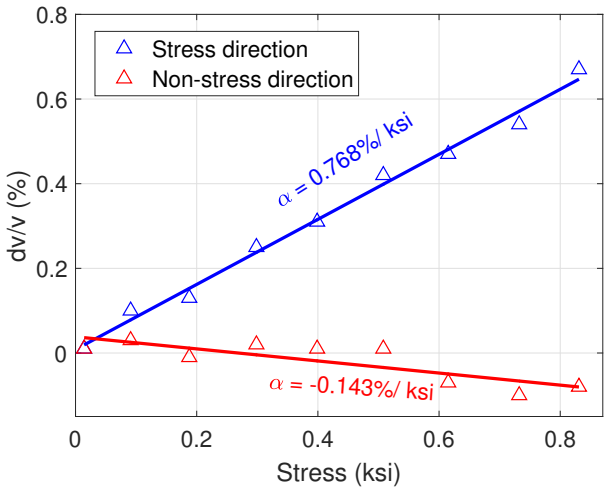

Fig. 3.11. Relative P wave velocity change vs. stress on the top surface of the 6" × 6" × 20" concrete beam.

Chapter 4

Test on a full-scale bridge girder

The proposed ultrasonic test method was validated on a full scale bridge girder to monitor the stress release process. Temperature effects on ultrasonic velocity were also further investigated on the stressed and unstressed directions.

4.1 Bridge girder description and experimental setup

Validation experiment was performed on a newly cast prestressed concrete girder to monitor the process of prestress release at the Omaha site of Coreslab Structure Inc. The bridge girder is 40 meter (131 ft) long, and the concrete compressive strength at the test time was 52 MPa (7.5 ksi). The side view and cross-sections of the girder are shown in figure 4.1 and figure 4.2. The girder had been covered and steam cured at high temperature to accelerate the early strength, then it was exposed to ambient temperature before prestress release. The prestressing release process was divided into two parts: 1) the top strands were cut one by one using cutting torch; 2) all bottom strands were released slowly with the hydraulic pump.

The ultrasonic test setup was installed on the bottom flange at the mid-span of the girder, where it had the highest losses. Because the bottom surface is inaccessible, all sensors were installed on the side of the bottom flange at the mid-span, including one PZT sensor (ultrasonic transmitter) and two AE sensors (// receiver and $\perp$ receiver) (figure 4.3). The distance between the transmitter and the receivers was 300 mm (12"). Three mechanical strain gauge (DEMEC) targets were installed close to the ultrasonic parallel receiver for measuring strain after prestress release (figure 4.3). Ultrasonic signals were acquired at a sampling rate of 40 MS/s, with an interval of 0.1 second throughout the prestressing release process. The DEMEC data were measured only before and after the release process.

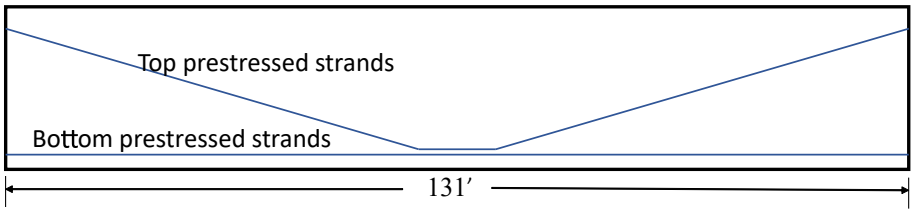

Fig. 4.1. Side view of the 131' prestressed concrete bridge girder (not to scale).

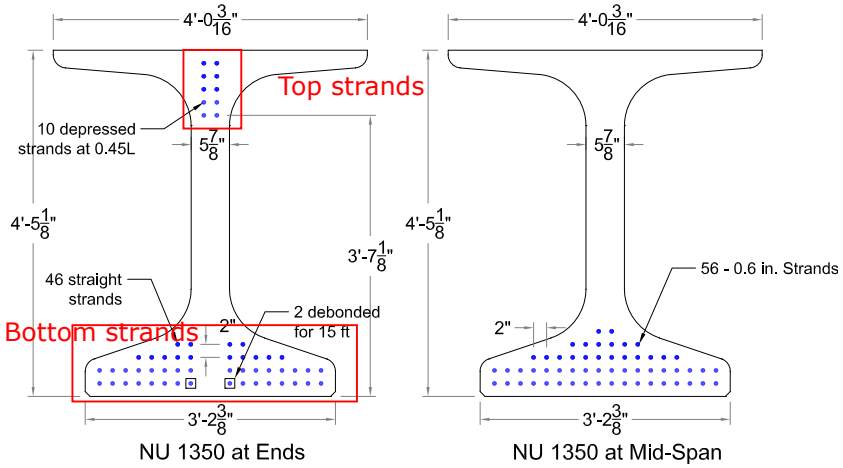

Fig. 4.2. Cross sections at the end (left) and middle (right) of the prestressed concrete bridge girder.

4.2 Results and discussion

4.2.1 Ultrasonic monitoring

The measured relative wave velocity changes in two directions are shown in figure 4.4(a), with the blue curve representing measurements in the prestress direction. The top strands were released one by one in the period of 40-150 seconds, and the bottom strands were released slowly in the period of 940-1335 seconds. The total P wave velocity change in the prestress direction was about 3% when the prestress release finished.

During the time gap between release of the top and the bottom strands (150-940 seconds) and after prestress release finished (> 1335 seconds), the velocities in both directions still showed slight increase with time although stress was constant during that period. We believe the slow velocity change after stress release was due to temperature effect when the concrete girder was exposed to cold ambient temperature after curing cover was removed. The temperature effect presented in the entire prestress release process. We can correct

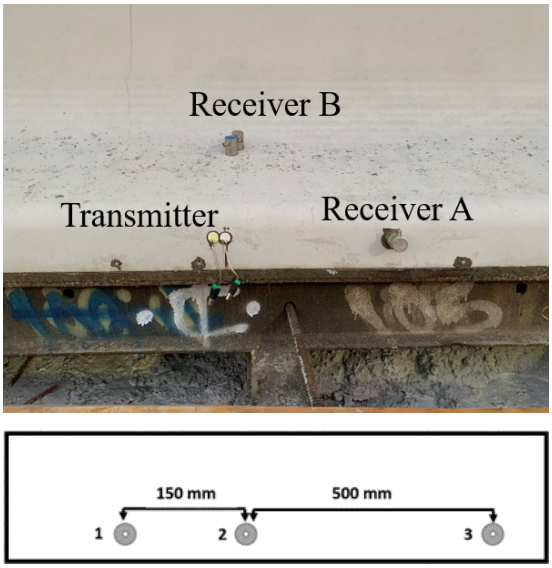

Fig. 4.3. Ultrasonic sensors (top) and DEMC target positions (bottom) on the bridge girder.

the temperature effect using the velocity change rate in the stress free period (t >1335 seconds). The relative velocity change after temperature correction is shown in figure 4.4(b). Similar to the small beam test in laboratory, the relative velocity changes in the longitudinal and transverse directions show opposite signs. The velocity in the transverse direction decreased during the release process due to Poisson's effect with relative change of -0.275% after temperature correction.

When we zoom in the segment of the top strands cutting (40-150 second), as shown in the inset in figure 4.4(b), the dv/v curve clearly recorded the step-wise process when the top strands were cut one by one. The bottom release shows a relative smooth process. These results indicate that the ultrasonic test not only recorded the change of wave velocity due to stress change, but also showed more details of the stress release process of the prestressed steel strands.

4.2.2 Stress and strain measurements

Strain measurement using DEMEC

In order to calculate the acoustoelastic coefficient, we need to measure the stress/strain change caused by prestress release. In this test, the total strain measured by the DEMEC was -0.083% in the entire prestress release process. The modulus of elasticity of concrete can be estimated using the following empirical formula adopted by AASHTO LRFD [31]:

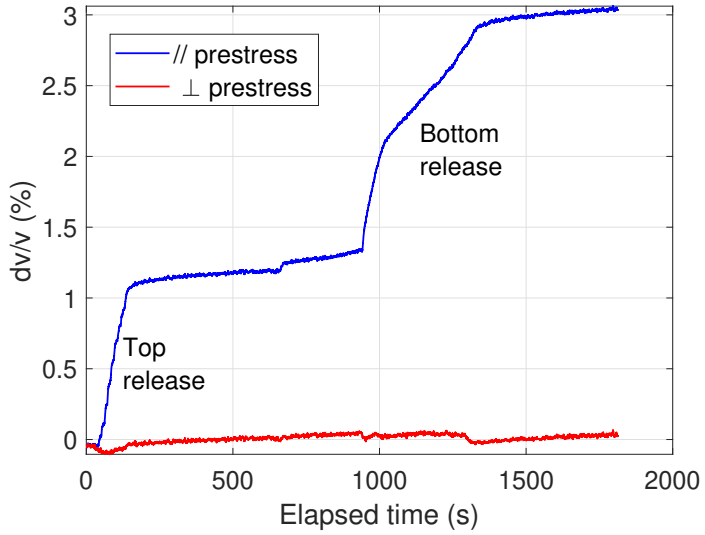

(a) Before temperature correction

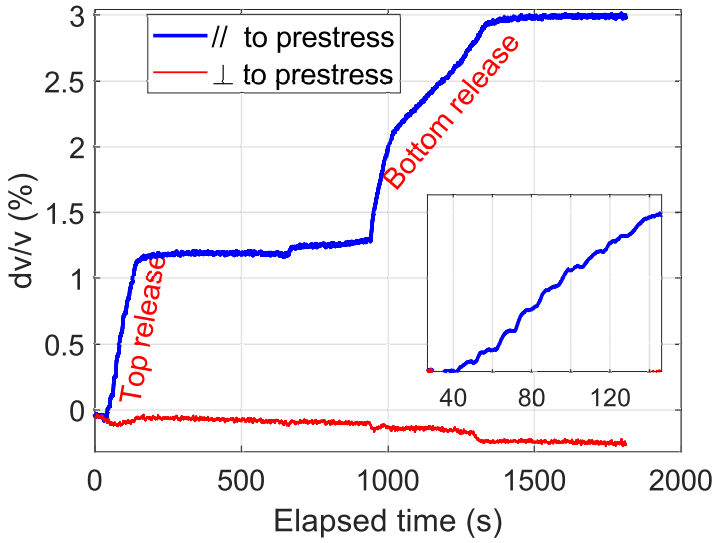

(b) After temperature correction

Fig. 4.4. Relative velocity change monitored during the prestress release process on the 131-ft long bridge girder, before and after temperature correction. Blue lines represent the result from the parallel receiver, and the red lines are from the perpendicular receiver. The inset in (b) shows more details in the process of cutting the top strands.

$$E_c = 33,000\gamma^{1.5}\sqrt{f_c'} \text{ (ksi)} \tag{4.1}$$

where

$$\gamma = \text{ unit weight of concrete (kcf)}$$
$$f_c' = \text{ concrete compressive strength (ksi)}$$

With the measured total strain of -0.083% from DEMEC data, the stress is then calculated as 28.3 MPa (4.1 ksi). The acoustoelastic coefficient in the stress direction is α = 0.731 %/ksi, and in the transverse direction is α = -0.007 %/ksi.

AASHTO LRFD Prestress Losses Calculations

The stress in concrete after prestress release can also be calculated based on AASHTO LRFD specifications [31]. The detailed calculation procedure is shown in figure 4.5. The calculated stress is 4.3 ksi, which is very close to the result 4.1 ksi based on DEMEC measurement.

4.3 Temperature effect in prestressed concrete members

4.3.1 prestressed concrete specimens and test setup

Temperature has significant influence on measurements of strain, camber, and ultrasonic wave velocity, and the temperature effects are often comparable to or even larger than the stress induced changes. The proposed self-reference ultrasonic test method provide a solution to reduce the effect of temperature substantially. In Figure 4.4(a), the wave velocities in both directions were affected by temperature change in the girder. Figure 4.4(b) gives the temperature corrected results using the data after prestress release (constant stress). Although the relative velocity changes have different values after correction, the difference between the velocities in two directions does not change. Therefore, as long as the concrete in test region has a uniform temperature distribution, we can always use the measurement in stress free direction as a reference.

However, the temperature induced wave velocity change may be different at different stress levels. That means the self-reference test method may only partially cancel the temperature effect on a prestressed concrete member, because the temperature induced velocity changes are slightly different in the prestress direction and unstressed direction .

AASHTO LRFD Prestress Losses Calculations

NU1350

Elastic Shortening Losses

Girder Span	$L := 131\ ft$
Girder Gross Area	$A_g := 753.5\ in^2$
Girder C.G from bottom	$y_b := 24\ in$
Girder Gross Inertia	$I_g := 302690\ in^4$
Compressive strength at Release	$f_{ci}' := 7.5\ ksi$
Girder Aggregate Factor	$k_1 := 1.0$
Girder MOE at Release	$E_{ci} := 33000\ ksi \cdot k_1 \cdot \left(\frac{145\ pcf}{1000\ pcf}\right)^{1.5} \cdot \left(\frac{f_{ci}'}{ksi}\right)^{.5} = 4990\ ksi$
Girder Weight	$q_g := A_g \cdot 150\ pcf = 0.785\ \frac{kip}{ft}$
Girder Weight Moment	$M_g := q_g \frac{L^2}{8} = 1683.7\ kip \cdot ft$
Strand Ultimate Srength	$f_{pu} := 270\ ksi$
Prestressing Prior to Transfer	$f_{pi} := 75\% \cdot f_{pu} = 202.5\ ksi$
Strand MOE	$E_p := 28500\ ksi$
Area of Prestressing Strands	$A_{ps} := 56 \cdot 0.217\ in^2 = 12.15\ in^2$
Eccentricity of Strands	$e_{pg} := 19.57\ in$
Elastic Shortening Loss	$\Delta f_{pES} := \frac{A_{ps} \cdot f_{pi} \cdot \left(I_g + {e_{pg}}^2 \cdot A_g\right) - e_{pg} \cdot A_g \cdot M_g}{A_{ps} \cdot \left(I_g + {e_{pg}}^2 \cdot A_g\right) + A_g \cdot I_g \cdot \frac{E_{ci}}{E_p}} = 24.6\ ksi$
Elastic Shortening Loss	$ES := \frac{\Delta f_{pES}}{f_{pi}} = 12.127\%$
Concrete Stress at Prestress C.G.	$f_{cgp} := \frac{E_{ci}}{E_p} \cdot \Delta f_{pES} = 4.3\ ksi$

Fig. 4.5. Prestress loss calculation based on AASHTO specifications.

To investigate the temperature effect on ultrasonic velocity in prestressed concrete members, we performed two experiments: one on a the prestressed concrete bridge girder at Coreslab Inc., and another on a one-way prestressed concrete slab in the structural laboratory at Perter Kiewit Institute (PKI), as shown in figure 4.6 and figure 4.7.

In the bridge girder test (figure 4.6), the ultrasonic sensors were installed on the bottom surface, with the transmitter and longitudinal receiver close to the edge, and the transverse receiver towards the inside. The distance between the transmitter and receivers was 12". Two thermocouple sensors were also attached to the bottom surface to monitor the temperature change of concrete. The monitoring lasted for about 6 hours from early morning to noon. The girder temperature increased from 23 °C to 28 °C. Although the sensors were installed on the bottom surface to avoid direct sunlight, there was still temperature gradient in concrete between the two thermocouples and along the transverse ultrasonic wave path.

Fig. 4.6. Investigating temperature effect on ultrasonic wave velocity in the bridge girder.

In the prestressed concrete slab test (figure 4.7), similar to the setup on the girder, one transmitter and two receivers were installed on the top surface in orthogonal directions. Two thermalcouple sensors were attached to the tested area to monitor the temperature change of the concrete slab in ambient condition. The test lasted for about 12 hour.

In both tests, the temperature data were measured and recorded by a Pico® TC-08 Thermocouple Data Logger. Since the temperature change was relatively slow, the ultrasonic signals and temperature data were collected every 10 minutes. A LabVIEW program was used to control the data acquisition system and synchronize ultrasonic data and temperature data.

Fig. 4.7. Test on an one-way prestressed concrete slab in PKI structural laboratory to investigate the temperature effect on the ultrasonic wave velocity in prestressed concrete members.

4.3.2 Results of temperature effect

Using the analysis method described in section 3.3, the relative velocity change dv/v caused by temperature are presented in figure 4.8 for the bridge girder and figure 4.9 for the prestressed concrete slab. In all tests, the wave velocities in both directions are affected by temperature and they decrease with increasing temperature. In the bridge girder test, the velocity change reached 0.35% in 5 °C temperature range.

The curves in two tests have different slopes, which are caused by different materials and temperature gradient. However, within each test, the velocity in the prestressed direction has a slightly smaller slope than in the unstressed direction. The slope difference between two directions is only $0.0235\,\%/\,^{o}\mathrm{C}$ in both tests. This difference can be explained by the nonlinear behavior of concrete material. When the concrete is prestressed, it becomes denser and has lower nonlinearity than in the unstressed condition. In the stressed direction, the velocity is also less sensitive to temperature change than in the unstressed direction.

If the prestress level is low, then the $dv/v \sim T$ slope difference between two directions is small, i.e., the temperature effects on velocity in both directions are almost equal. The self-reference test setup will automatically cancel the temperature effect by measuring the velocity difference between two directions. When the prestress level is high, as in the case of the bridge girder test, using the self-reference setup will still be able to reduce the 70% to 80% of temperature induced measurement error. The remaining temperature effect can be further compensated by using the slope difference between two directions.

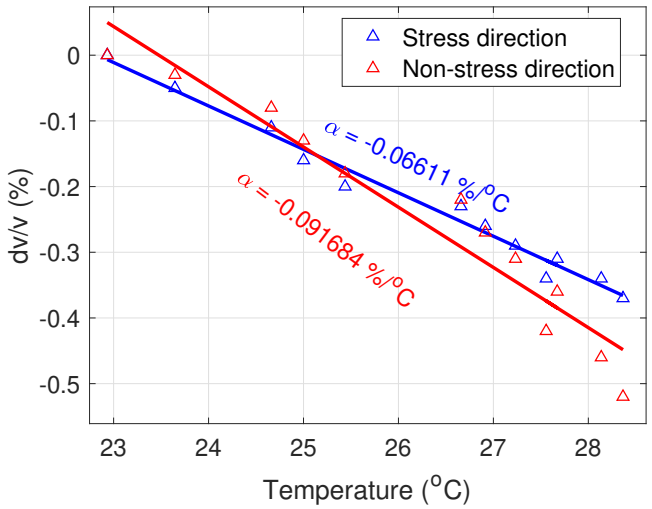

Fig. 4.8. Relative velocity change with temperature on the prestressed concrete bridge girder.

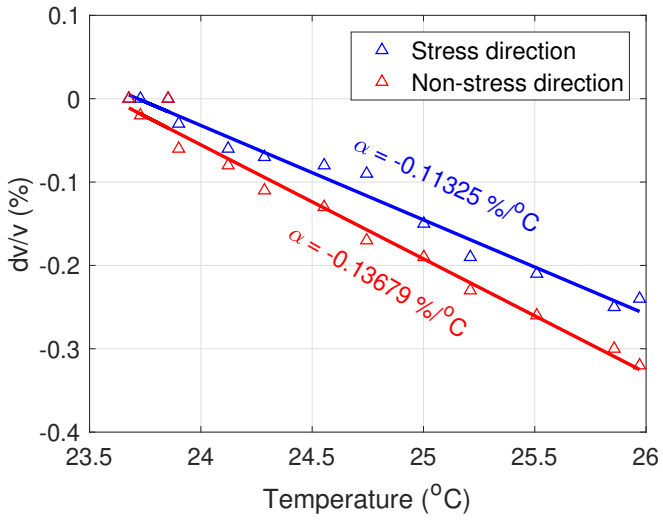

Fig. 4.9. Relative velocity change with temperature on the one-way prestressed concrete slab.

Chapter 5

Conclusions and future work

In this study, we experimentally investigated the ultrasonic acoustoelastic effects in concrete, using small scale specimens and full-size prestressed concrete bridge girders. Accurate wave velocity measurements are needed in order to estimate prestress loss using this technique. Coda wave interferometry (CWI) is commonly used for analysis of small wave velocity change in concrete. Our study showed the results from CWI analysis are strongly affected by the time window position in signals. We proposed to only use the direct P-wave part in the time range of $[t_p, 1.5t_p]$ for CWI analysis and obtained consistent results.

In both the small beam and big girder tests, along the direction parallel to the applied stress, the wave velocity increases with compressive stress level and shows highest sensitivity to stress change. In the transverse direction (no stress), the velocity decreases with stress due to Poisson's effect and it has the lowest sensitivity.

The proposed ultrasonic method was validated on a 131-ft long prestressed concrete girder at Coreslab Structures in Omaha. We monitored the entire prestress release process using ultrasonic waves. The ultrasonic method clearly shows the stress release process and indicates each strand cut detail. The measured acoustoelastic is 0.731%/ ksi in the prestressed concrete girder, similar to the value obtained in laboratory specimens.

We also investigated the temperature effect on ultrasonic wave velocity in prestressed concrete members. Although temperature has significant effect on wave velocity measurement, the proposed self-reference test setup can effectively cancel or compensate the temperature effect by using the velocity measurement in the unstressed direction as the reference.

This phase I research proved the feasibility of using ultrasonic waves for evaluation of prestress loss in prestressed concrete girders. Camber is another important parameter in construction and placement of prestressed concrete girders. The future work will be focused

on prediction of prestress loss and camber growth of prestressed concrete girders during the period from release to deck construction. In order to apply this NDT technique to practice, the future works include:

1. build the relationship between ultrasonic wave velocity and strain in concrete based on measurements on Nebraska prestressed concrete girders;
2. develop an instrument and algorithm capable of measuring wave velocity differences with high accuracy;
3. understand and correct temperature effects on ultrasonic and camber measurements;
4. develop a calculation procedure to predict stress loss and camber from production to deck placement based on ultrasonic measurement;
5. improve the current camber calculation procedure by measuring actual modulus of elasticity E using ultrasonic waves before prestress release.

Bibliography

[1] E. Baran, C. Shield, and C. French, "A comparison of methods for experimentally determining prestress losses in pretensioned prestressed concrete girders," *American Concrete Institute (ACI) Special Publication on Historic Innovations in Prestressed Concrete (SP-231)*, pp. 161–180, 2005.

[2] J. R. Martí-Vargas, L. Caro, and P. Serna, "Experimental technique for measuring the long-term transfer length in prestressed concrete," *Strain*, vol. 49, no. 2, pp. 125–134, 2013.

[3] I. Lillamand, J.-F. Chaix, M.-A. Ploix, and V. Garnier, "Acoustoelastic effect in concrete material under uni-axial compressive loading," *NDT & E International*, vol. 43, no. 8, pp. 655–660, 2010.

[4] T. Planès and E. Larose, "A review of ultrasonic coda wave interferometry in concrete," *Cement and Concrete Research*, vol. 53, pp. 248–255, 2013.

[5] K. F. Bompan and V. G. Haach, "Ultrasonic tests in the evaluation of the stress level in concrete prisms based on the acoustoelasticity," *Construction and Building Materials*, vol. 162, pp. 740–750, 2018.

[6] E. Larose and S. Hall, "Monitoring stress related velocity variation in concrete with a 2× 10- 5 relative resolution using diffuse ultrasound," *The Journal of the Acoustical Society of America*, vol. 125, no. 4, pp. 1853–1856, 2009.

[7] Y. Zhang, O. Abraham, V. Tournat, A. Le Duff, B. Lascoup, A. Loukili, F. Grondin, and O. Durand, "Validation of a thermal bias control technique for coda wave interferometry (CWI)," *Ultrasonics*, vol. 53, no. 3, pp. 658–664, 2013.

[8] C. Payan, V. Garnier, J. Moysan, and P. Johnson, "Determination of third order elastic

constants in a complex solid applying coda wave interferometry," *Applied Physics Letters*, vol. 94, no. 1, p. 011904, 2009.

[9] D. P. Schurr, J.-Y. Kim, K. G. Sabra, and L. J. Jacobs, "Damage detection in concrete using coda wave interferometry," *NDT & E International*, vol. 44, no. 8, pp. 728–735, 2011.

[10] A. Tourin, A. Derode, A. Peyre, and M. Fink, "Transport parameters for an ultrasonic pulsed wave propagating in a multiple scattering medium," *The Journal of the Acoustical Society of America*, vol. 108, no. 2, pp. 503–512, 2000.

[11] S. C. Stähler, C. Sens-Schönfelder, and E. Niederleithinger, "Monitoring stress changes in a concrete bridge with coda wave interferometry," *The Journal of the Acoustical Society of America*, vol. 129, no. 4, pp. 1945–1952, 2011.

[12] E. Larose, J. de Rosny, L. Margerin, D. Anache, P. Gouedard, M. Campillo, and B. van Tiggelen, "Observation of multiple scattering of khz vibrations in a concrete structure and application to monitoring weak changes," *Physical Review E*, vol. 73, no. 1, p. 016609, 2006.

[13] E. Niederleithinger and C. Wunderlich, "Influence of small temperature variations on the ultrasonic velocity in concrete," in *AIP Conference Proceedings*, vol. 1511, pp. 390–397, AIP, 2013.

[14] Y. Zhang, O. Abraham, E. Larose, T. Planes, A. Le Duff, B. Lascoup, V. Tournat, R. El Guerjouma, L.-M. Cottineau, and O. Durand, "Following stress level modification of real size concrete structures with coda wave interferometry (CWI)," in *AIP Conference Proceedings*, vol. 1335, pp. 1291–1298, 2011.

[15] H. Sun and J. Zhu, "Thermal modulation of nonlinear ultrasonic wave for concrete damage evaluation," *The Journal of the Acoustical Society of America*, vol. 145, no. 5, pp. EL405–EL409, 2019.

[16] F. D. Murnaghan, *Finite deformation of an elastic solid*. Wiley, 1951.

[17] D. S. Hughes and J. Kelly, "Second-order elastic deformation of solids," *Physical review*, vol. 92, no. 5, p. 1145, 1953.

[18] D. Egle and D. Bray, "Measurement of acoustoelastic and third-order elastic constants for rail steel," *The journal of the Acoustical Society of America*, vol. 60, no. 3, pp. 741–744, 1976.

[19] O. I. Lobkis and R. L. Weaver, "Coda-wave interferometry in finite solids: Recovery of p-to-s conversion rates in an elastodynamic billiard," *Physical Review Letters*, vol. 90, no. 25, p. 254302, 2003.

[20] R. Snieder, A. Grêt, H. Douma, and J. Scales, "Coda wave interferometry for estimating nonlinear behavior in seismic velocity," *Science*, vol. 295, no. 5563, pp. 2253–2255, 2002.

[21] C. Hadziioannou, E. Larose, O. Coutant, P. Roux, and M. Campillo, "Stability of monitoring weak changes in multiply scattering media with ambient noise correlation: Laboratory experiments," *The Journal of the Acoustical Society of America*, vol. 125, no. 6, pp. 3688–3695, 2009.

[22] E. Niederleithinger, X. Wang, M. Herbrand, and M. Müller, "Processing ultrasonic data by coda wave interferometry to monitor load tests of concrete beams," *Sensors*, vol. 18, no. 6, p. 1971, 2018.

[23] R. Snieder, "Coda wave interferometry and the equilibration of energy in elastic media," *Physical Review E*, vol. 66, no. 4, p. 046615, 2002.

[24] P. Fröjd and P. Ulriksen, "Frequency selection for coda wave interferometry in concrete structures," *Ultrasonics*, vol. 80, pp. 1–8, 2017.

[25] I. Shkolnik, "Effect of nonlinear response of concrete on its elastic modulus and strength," *Cement and Concrete Composites*, vol. 27, no. 7-8, pp. 747–757, 2005.

[26] H. Akaike, "A bayesian analysis of the minimum aic procedure," *Annals of the Institute of Statistical Mathematics*, vol. 30, pp. 9–14, Dec 1978.

[27] N. Maeda, "A method for reading and checking phase time in auto-processing system of seismic wave data," *Zisin (Journal of the Seismological Society of Japan. 2nd ser.)*, vol. 38, no. 3, pp. 365–379, 1985.

[28] P. Jousset, C. Haberland, K. Bauer, and K. Arnason, "Hengill geothermal volcanic complex (iceland) characterized by integrated geophysical observations," *Geothermics*, vol. 40, no. 1, pp. 1–24, 2011.

[29] M. Kotsovos, "Effect of testing techniques on the post-ultimate behaviour of concrete in compression," *Materials and Structures*, vol. 16, no. 1, pp. 3–12, 1983.

[30] S. Kumar, T. Mukhopadhyay, S. Waseem, B. Singh, and M. Iqbal, "Effect of platen restraint on stress–strain behavior of concrete under uniaxial compression: a comparative study," *Strength of Materials*, vol. 48, no. 4, pp. 592–602, 2016.

[31] American Association of State Highway and Transportation Officials (AASHTO), *AASHTO LRFD Bridge Design Specifications (8th Edition)*. Washington, DC: AASHTO, 2017.